Supporting Material

Interactions of the Anticancer Drug Tamoxifen with Lipid Membranes

Nawal Khadka[1], Xiaolin Cheng[2,3], Chian-Sing Ho[1], John Katsaras[4,5,6], and Jianjun Pan[1]*

[1]Department of Physics, University of South Florida, Tampa, FL 33620, USA

[2]Computer science and Mathematics Division, Oak Ridge National Laboratory, Oak Ridge, TN 37831, USA

[3]Department of Biochemistry and Cellular and Molecular Biology, University of Tennessee, Knoxville, TN 37996, USA

[4]Neutron Sciences Directorate, Oak Ridge National Laboratory, Oak Ridge, TN 37831, USA

[5]Department of Physics and Astronomy, University of Tennessee, Knoxville, TN 37996, USA

[6]Joint Institute for Neutron Sciences, Oak Ridge National Laboratory, Oak Ridge, TN 37831, USA

1. SANS data

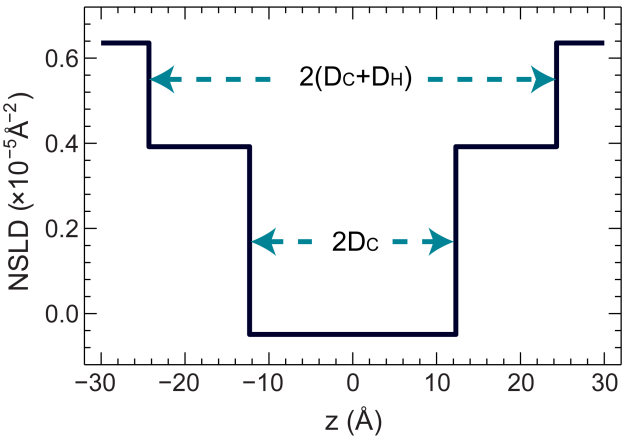

Figure S1 Schematic of the 3-strip model, in which the lipid bilayer's hydrocarbon core, lipid headgroup, and bulk water are each described by strips with constant neutron scattering length densities (NSLDs). Specifically, the hydrocarbon core is represented by $2D_C$, and is flanked by the headgroup strip located between D_C and D_C+D_H. The bulk water strip resides adjacent to the headgroup. Due to water impermeability, the central strip's NSLD (ρ_C) is independent of D_2O concentration. This is in contrast to the hydrophilic headgroup, which is described by a second strip of width D_H. The NSLD in this region (ρ_H) is the sum of the lipid headgroup and its associated water molecules. As a result, ρ_H is dependent on the bulk water NSLD (ρ_{water}). Overall, the 3-strip model at three D_2O concentrations is described by six free parameters, including the thickness ($2D_C$) and NSLD (ρ_C) of the hydrocarbon core, the headgroup's thickness (D_H), and the headgroup's three NSLDs.

The scattering intensity based on the 3-strip model (S1) can be expressed as:

$$I = \left[2D_C(\rho_C - \rho_H)\,\mathrm{sinc}(qD_C) + 2(D_C + D_H)(\rho_H - \rho_{\mathrm{water}})\,\mathrm{sinc}[q(D_C + D_H)]\right]^2 ,$$

where $\mathrm{sinc}(x)=\sin(x)/x$; ρ_H, ρ_C and ρ_{water} are NSLD for lipid headgroup, hydrocarbon core and bulk water, respectively. The best fitting parameters for a POPC/POPG bilayer with 0 and 10 mol% TAM are shown in Table S1. Note that the D_H values are overestimated, a problem noted previously (S1). Therefore, we will only focus on $2D_C$ when discussing bilayer thickness changes induced by TAM.

Table S1 Structural parameters for POPC/POPG and POPC/POPG/TAM bilayers based on 3-strip model fits to SANS data.

	POPC/POPG	**POPC/POPG/TAM**
$2D_C$ (Å)	24.6±0.2	27.4±0.2
D_H (Å)	12.0±0.1	13.4±0.1
ρ_C (10^{-5} Å^{-2})	-0.049±0.006	-0.049±0.002
ρ_H (100% D_2O) (10^{-5} Å^{-2})	0.392±0.002	0.485±0.006
ρ_H (75% D_2O) (10^{-5} Å^{-2})	0.296±0.002	0.358±0.004
ρ_H (50% D_2O) (10^{-5} Å^{-2})	0.201±0.001	0.222±0.003

2. MD simulations

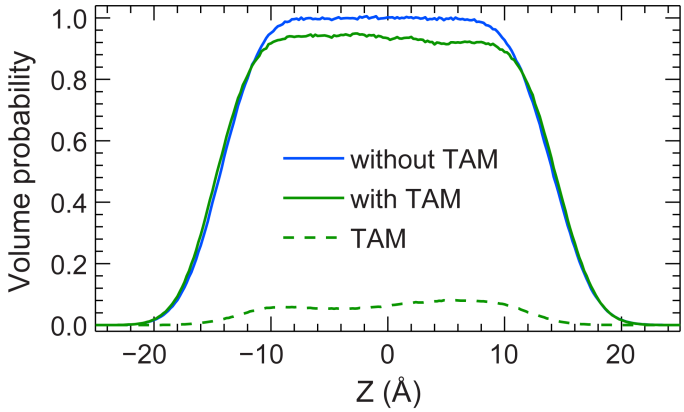

Figure S2 Volume probabilities calculated from MD simulations. The solid lines are volume probabilities for lipid hydrocarbon chains (including POPC and POPG) without (blue line) and with 10 mol% (green line) TAM. The decreased volume probability for the lipid chains with TAM is due to the presence of the TAM, whose volume probability is shown by the dashed line. Model fitting using a pair of error functions (S2, S3) indicates the hydrocarbon chain thickness $2D_C$ is 28.5 Å for the bilayer without TAM, and 29.3 Å for the bilayer with TAM. The addition of TAM increases the hydrocarbon chain thickness by 0.8 Å. This value is smaller than that obtained from SANS data analyses. This is not surprising considering the crude model used to analyze SANS data. Based on our MD simulations, the hydrocarbon chain volume V_{chain} is 922.5 and 925.4 $Å^3$ for bilayers without and with TAM, respectively. Using the relation of lipid area $A = V_{chain}/D_C$, the average lipid area is 64.8 and 63.2 $Å^2$ for bilayers without and with TAM, respectively.

Table S2 Structural parameters obtained from MD simulations for a POPC/POPG bilayer with 0 and 10 mol% TAM. V_{chain} is the lipid hydrocarbon chain volume; $2D_C$ is the bilayer hydrocarbon chain thickness; and A_{lipid} is the average lipid area. Atom number densities are directly calculated from MD simulations. Using the principle that the total volume probability at each slice Z equals unity (S4), V_{chain} is calculated. To obtain $2D_C$, the total volume probability of lipid hydrocarbon chains (Fig. S2) is fitted using a pair of error functions (S2, S3):

$$f(Z)=\frac{1}{2}\left[\mathrm{erf}\left(\frac{Z+D_C}{\sqrt{2}\sigma}\right)-\mathrm{erf}\left(\frac{Z-D_C}{\sqrt{2}\sigma}\right)\right],\quad \mathrm{erf}(Z)=\frac{2}{\sqrt{\pi}}\int_0^Z \exp\left(-t^2\right)dt$$

The average lipid area A_{lipid} is obtained using the box relation: $A_{lipid}=V_{chain}/D_C$. Averaged values of the two sets of simulations are also listed.

	Set 1		Set 2		Average	
	POPC/POPG	POPC/POPG/TAM	POPC/POPG	POPC/POPG/TAM	POPC/POPG	POPC/POPG/TAM
V_{chain} ($Å^3$)	920.5	928.7	924.4	922.1	922.5	925.4
$2D_C$ (Å)	28.4	29.3	28.6	29.3	28.5	29.3
A_{lipid} ($Å^2$)	64.8	63.3	64.7	63.0	64.8	63.2

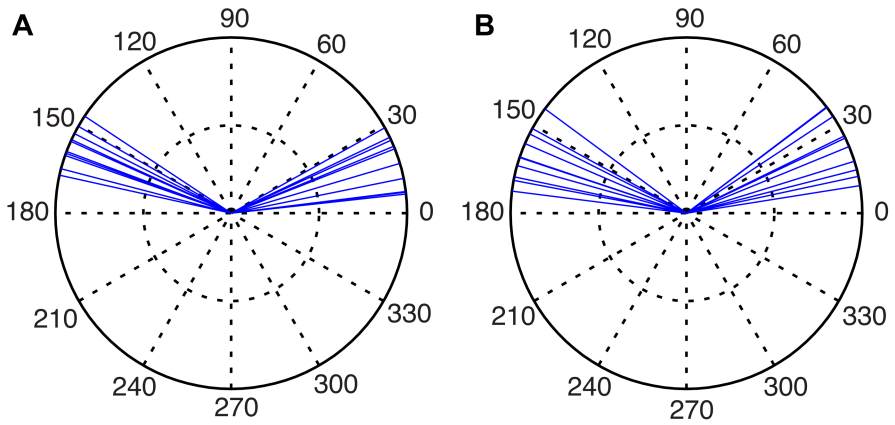

Figure S3 Initial angles of the O-C11 vectors for the 20 TAM molecules used in simulation set 1 (A) and set 2 (B). The vectors are oriented in a range of 7°-38° in one bilayer leaflet, and 142°-172° in the opposite bilayer leaflet.

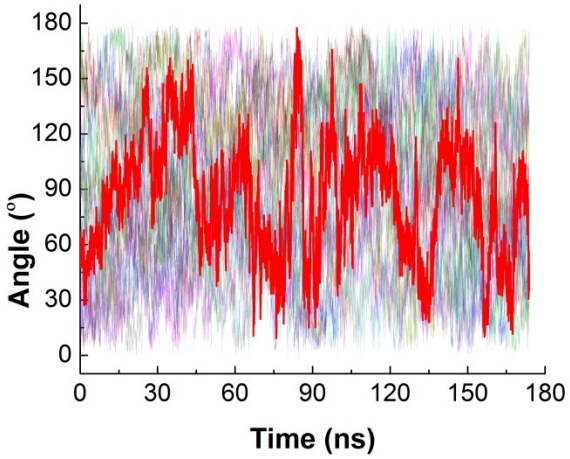

Figure S4 Time trajectories of the orientational angles for the 20 TAM molecules during our simulation. The orientation for each TAM molecule is defined as the angle between the vector connecting the oxygen and C11 atoms (O-C11) of TAM with respect to the bilayer normal. One selected trajectory is highlighted in red. The vector angles oscillate between 30° and 150°, highlighting the dynamic conformation of TAM within the lipid bilayer.

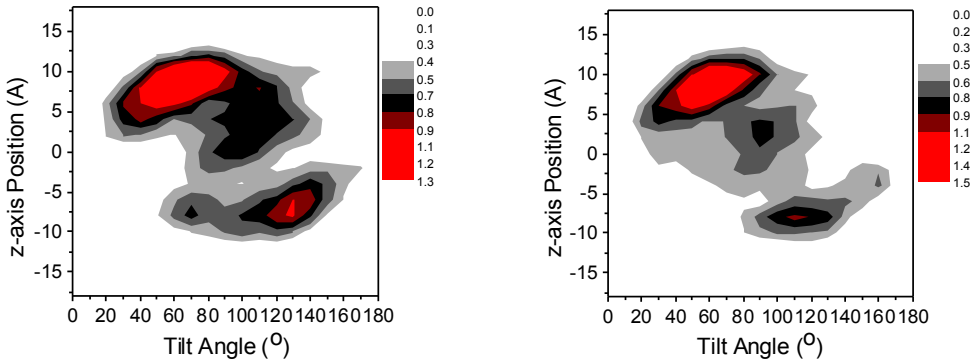

Figure S5 Correlation of TAM position and orientation. The 2-dimensional surface plots show probability distributions of the Z-axis position of the C11 atom, and the tilt angle of the vector O-C11 (with respect to the bilayer normal) of the 20 TAM molecules. The left and right figures are calculated from two sets of simulations using different simulation methods (see main text for details). A clear correlation between the position and the tilt angle is observed. For the Z-position ranging from 5 to 10 Å, the most probable tilt angles are distributed between 20° and 90°. As the C11 atom moves toward the bilayer center (i.e., Z ~ 0 Å), the most probable angles are confined to a region centered near 90°. Note that the asymmetry between the upper left and the lower right regions are most likely due to the relatively small size of our simulations.

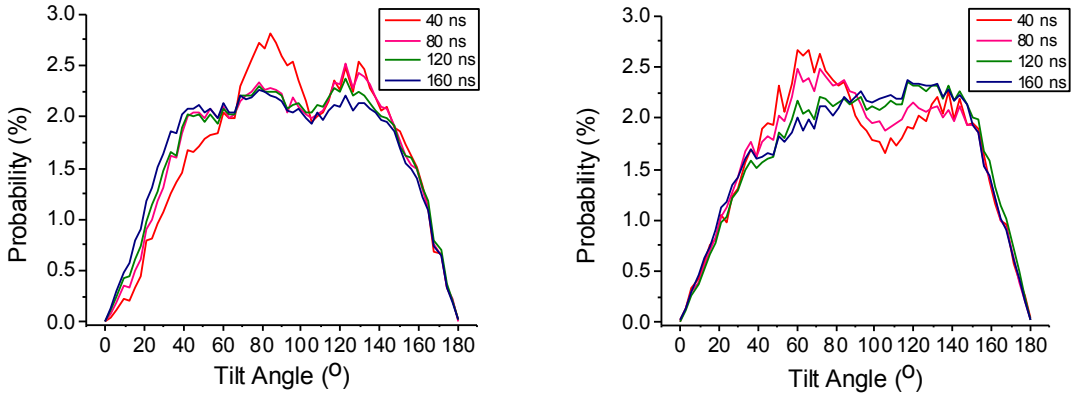

Figure S6 Time-block averaged TAM angle distributions of the vector O-C11 with respect to the bilayer normal within the POPC/POPG bilayer, constructed from two sets of simulations (left and right) using different simulation methods. For each set, the 120 ns block (80 to120 ns) overlaps well with the 160 ns block (120 to 160 ns). This supports the convergence of our simulations. Overall, the O-C11 vector displays broad angular distribution, with the largest probabilities occurring between 30° and 150°.

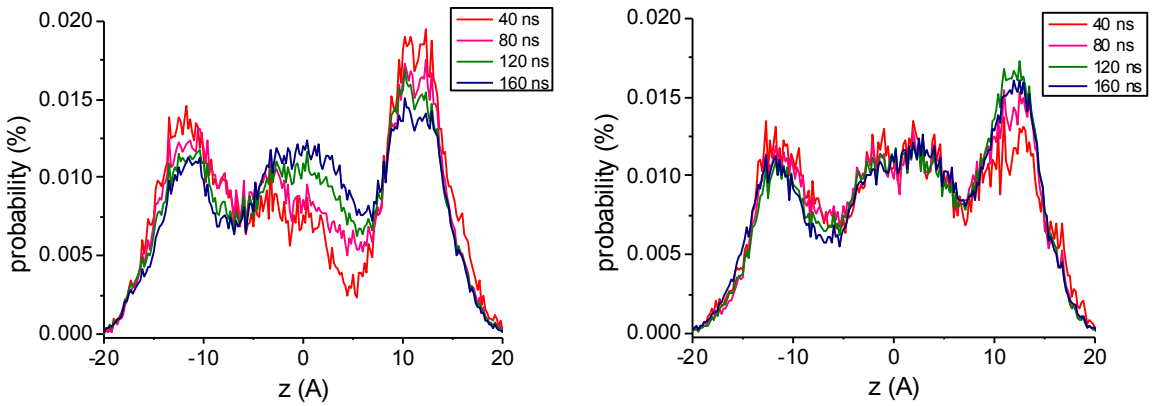

Figure S7 Time-block averaged positional distributions of the TAM nitrogen atom (N-TAM) within the POPC/POPG bilayer, constructed from two sets of simulations (left and right) using different simulation methods. It is clear that the distribution overlaps well for the 120 ns block (80ns to120 ns) and the 160 ns block (140 ns to 160 ns), supporting the convergence of our simulations.

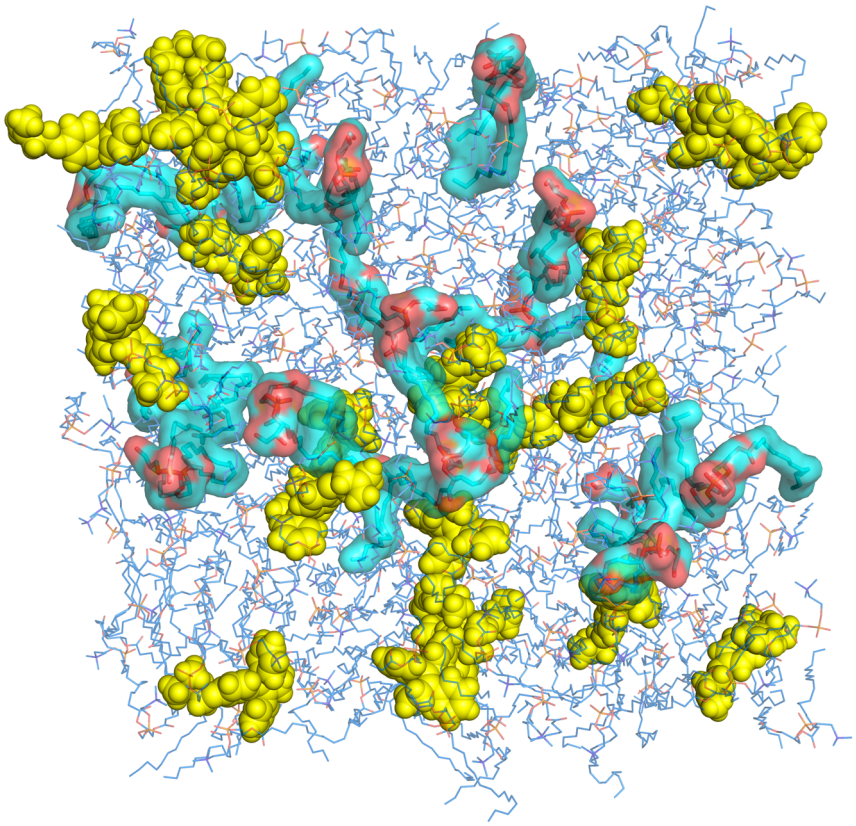

Figure S8 Top view of an equilibrated POPC/POPG/TAM bilayer from our MD simulations. TAM molecules are represented by yellow spheres; POPG lipids are represented by semitransparent surfaces with carbon atoms in cyan color; and POPC molecules are shown in line representation with carbon atoms in blue color. No specific association of TAM to either POPC or POPG lipids is observed, a result consistent with the fact that TAM molecules are located in the hydrocarbon chain region, and POPG and POPC have the same hydrocarbon chain composition.

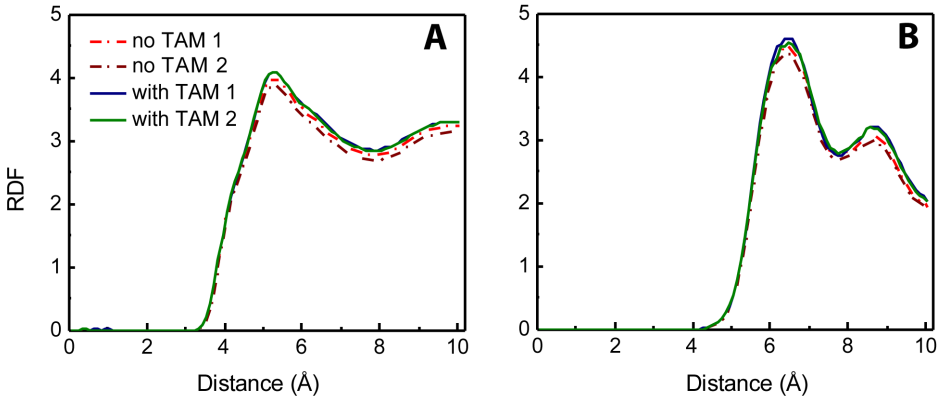

Figure S9 (A) Volume averaged radial distribution function (RDF) for the 15th carbon of the oleoyl chain with other acyl chain carbons (15th). (B) RDF of phosphorus-phosphorus in the headgroup region. Two sets of simulations for each bilayer system with and without TAM.

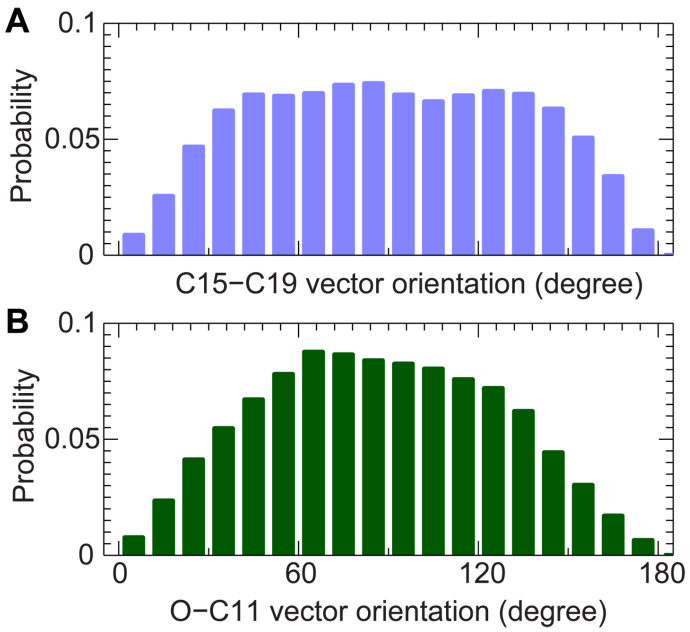

Figure S10 Orientational distributions of the two vectors C15-C19 (A) and O-C11 (B) with respect to the bilayer normal.

.

3. Atomic force microscopy experiments

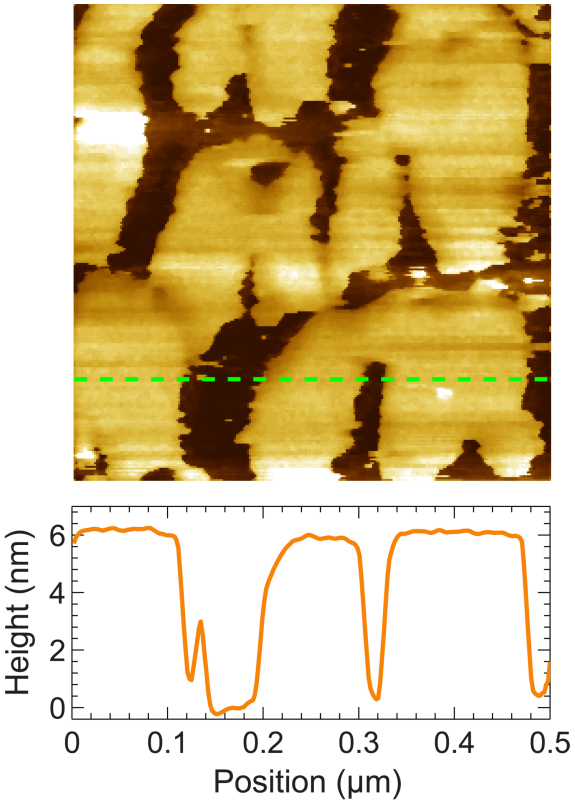

Figure S11 A partially formed solid supported POPC/POPG bilayer (0.5 μm × 0.5 μm). The height profile along the green dashed line is shown in the bottom panel. It is clear that the bilayer surface protrudes by ~ 6.0 nm above the mica substrate.

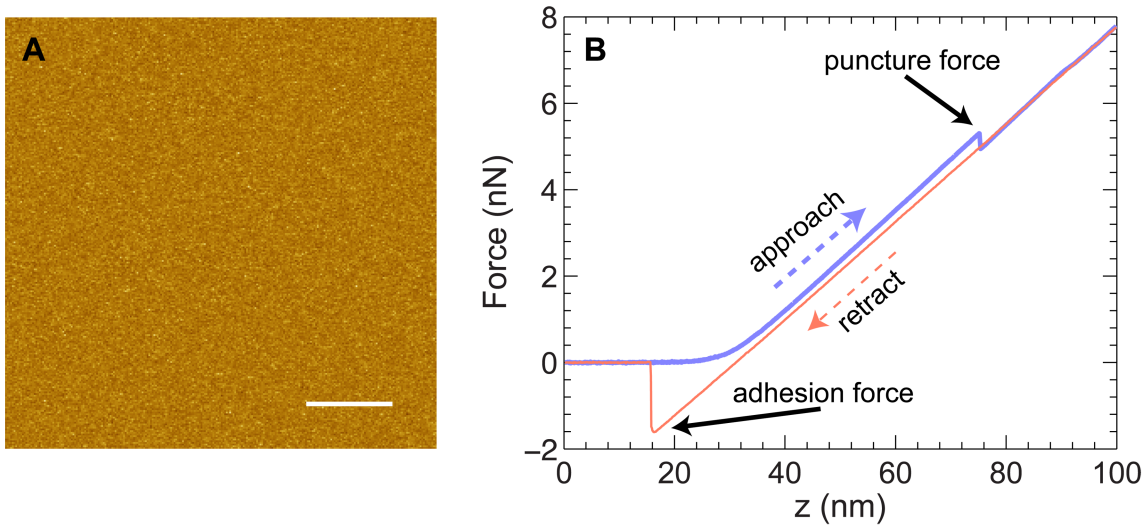

Figure S12 (A) A bilayer patch used for force spectroscopy measurements. Scale bar is 100 nm. (B) A pair of force-distance curves as the AFM tip approaches (blue line) and retracts from (orange line) a solid supported POPC/POPG bilayer. The puncture force is the largest force the bilayer can withstand before being punched through. An adhesion force is observed as the tip moves away from the bilayer. Note the hysteresis between the two force curves.

4. Vesicle leakage by fluorescence spectroscopy

Calcein-encapsulated unilamellar vesicles (ULVs) preparation. Lipid dry films were hydrated using HEPES buffer A (20 mM HEPES, 20 mM NaCl and 1 mM EDTA at pH 7.0) containing 30 mM water soluble and membrane impermeable fluorophore calcein. Freeze-thaw cycles between -80°C and 50°C were carried out to ensure uniform distribution of calcein across the multilamellar vesicles (MLVs). The resultant lipid solution was extruded using an Avanti mini-extruder outfitted with a 100 nm diameter pore filter to produce ULVs. A gel filtration column (Superdex 200 10/300 GL) was used to remove exterior calcein. The elution buffer contained 20 mM HEPES, 108 mM NaCl and 1 mM EDTA at pH 7.0 (HEPES buffer B). The vesicle portion was monitored by UV absorption at 280 nm using an ÄKTA pure (GE Healthcare, Piscataway, NJ). An example of the elution curve is shown in Fig. S12A. Due to size differences, calcein-encapsulated vesicles were eluted near 7.6 ml, while non-encapsulated calcein molecules were eluted near 20 ml. The equality of the osmotic pressure in the interior and at the exterior of calcein-encapsulated ULVs was confirmed using a Wescore 5500 vapor pressure osmometer (Logan, Utah). Lipid concentration in the eluted vesicle solution (~ 5 mM) was determined using a phosphorus assay kit from Abnova (Walnut, CA), and a PerkinElmer Lambda 950 spectrophotometer (Waltham, MA).

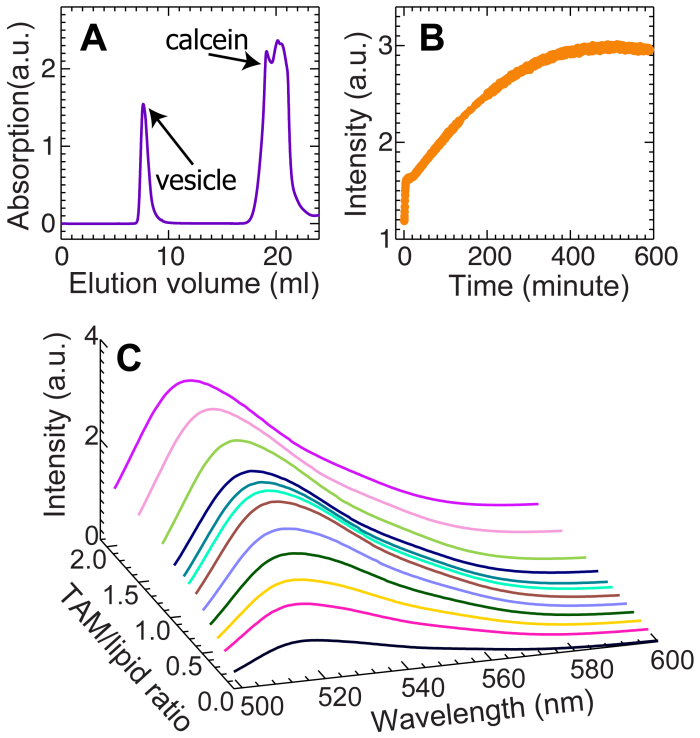

Figure S13 Leakage of calcein-encapsulated ULVs induced by TAM. (A) Size exclusion chromatography is used for separating vesicle-encapsulated calcein from exterior calcein. The vesicle fraction is eluted near 7.6 ml, and the exterior calcein near 20 ml. (B) An example of a time-course fluorescence measurement of calcein-encapsulated ULVs induced by TAM at a TAM/lipid ratio of 1.0. At the outset, fluorescence intensity increases rapidly, up to 9 minutes when it starts to increase more gradually. Maximum fluorescence intensity is attained after the ULVs were incubated for about 8 hours. (C) Fluorescence spectrum as a function of TAM/lipid ratio r. The excitation wavelength is 494 nm, and the excitation spectrum was collected from 498 nm to 600 nm. The maximum intensity is located near 514 nm for all curves.

Reference

S1. Pencer, J., S. Krueger, C. P. Adams, and J. Katsaras. 2006. Method of separated form factors for polydisperse vesicles. J Appl Crystallogr 39:293-303.

S2. Kučerka, N., J. F. Nagle, J. N. Sachs, S. E. Feller, J. Pencer, A. Jackson, and J. Katsaras. 2008. Lipid bilayer structure determined by the simultaneous analysis of neutron and X-ray scattering data. Biophys J 95:2356-2367.

S3. Pan, J. J., X. L. Cheng, L. Monticelli, F. A. Heberle, N. Kucerka, D. P. Tieleman, and J. Katsaras. 2014. The molecular structure of a phosphatidylserine bilayer determined by scattering and molecular dynamics simulations. Soft Matter 10:3716-3725.

S4. Petrache, H. I., S. E. Feller, and J. F. Nagle. 1997. Determination of component volumes of lipid bilayers from simulations. Biophys J 72:2237-2242.